A Reconstruction-registration Integrated Data Fusion Method for Measurement of Multi-scaled Complex Surfaces

Ming Jun Ren, Li Jian Sun, Ming Yu Liu, Chi Fai Cheung, Yue Hong Yin

***Abstract*—The combined use of multiple measurement sensors is considered as a promising solution in surface metrology. Such hybrid instruments require sophisticated data fusion process to achieve overall better measurement results. This paper presents a reconstruction-registration integrated data fusion method to address the difficulty in modelling and fusing multi-scaled complex datasets. The method decomposes the datasets into different scales by fitting a common surface via reconstruction and registration process so that the modelling and fusion process are also decomposed, and are only performed among the fitting and matching residuals of the datasets. The quality of the fused results are improved based on weighted mean method with the aid of Gaussian process model by taking into account the associated errors of each datasets. The validity of the proposed method is verified through a series of comparison tests with existing methods by both computer simulation and actual measurement. It is shown that both enhanced registration accuracy and fusion quality are achieved by the proposed method with acceptable computation cost. The method should improve the metrological performance of the multi-sensor instruments in measuring complex surfaces.**

Index Terms—Precision surface measurement, multi-scaled surfaces, surface registration, data fusion.

I. INTRODUCTION

The trend towards product miniaturisation constitutes a driving force for the application of complex surfaces in many fields such as advanced optics [1]. An emerging consequence is the use of patterns and structures e.g. micro lens arrays and micro pyramid on surfaces [2]. These advanced surfaces integrate several different scales of features which are used to realize specific functionalities of the products [3]. As

Ming Jun Ren, Lijian Sun, Yue Hong Yin is with the Institute of Robotics, School of Mechanical Engineering, Shanghai Jiao Tong University, Shanghai, China.
Ming Yu Liu, Chi Fai Cheung is with Partner State Key Laboratory of Ultra-precision Machining Technology, Department of Industrial and Systems Engineering, The Hong Kong Polytechnic University, Hong Kong

these advanced surfaces increasingly enter the marketplace, precision surface measurement becomes a stringent technology for the quality control of these surfaces.

Many measuring principles and instruments have been proposed and developed to cover a wide measurement range with respect to specific and varying metrological needs [4, 5]. For instance, micro and nano coordinate measuring machines, micro topography measuring instruments, interferometric based instruments, scanning electron microscopy (SEM), and so on. Most of these instruments have their own technological merits, and relatively few of them are able to fulfill all the required tasks and rendering multi-scale 3D measurement with high precision. As a result, multi-sensor metrology becomes a compromising solution for versatile measurement tasks. The idea is to integrate several different sensors into a unified system so as to measure the components such that the measurement range, efficiency, and accuracy can be improved. For example, Werth VideoCheck UA 400 [6] integrates imaging sensor, tactile scanning sensor, and white light sensor into a single system which is capable of measuring complex 3D geometries with sub-micrometric accuracy. WITec GmbH [7] integrates confocal Raman microscopy, atomic force microscopy and scanning near-field optical microscopy so as to perform relatively fast measurement of large-area samples. Data fusion is a further step of sensor integration. The measured datasets in multi-sensor systems may come from different spaces with different scales, resolutions, and associated uncertainties [9]. This makes the data fusion as a core step to fuse these datasets to produce a unified representation of the measured parts with improved reliability. Although multi-sensor fusion is an emerging technology in the fields of signal and image processing, robotics, and sensor network [9, 10], relatively little research work has been found in coordinate measurements.

In coordinate measurement, the process of data fusion can basically be divided into three steps which include pre-processing, registration, and fusion [9]. In pre-processing, all the measured datasets are transferred to a common and appropriate representation format for further processing. In registration, all the datasets are transformed to a common coordinate frame based on rigid motion. Iterative closest point (ICP) and its variants are the most widely used methods in the registration of the discrete datasets [11]. Fusion is responsible for processing the redundant data in the overlapping area of the datasets so as to produce a unique representation. Considering the fused datasets may have different resolutions with different associated uncertainties, proper fusion process should be carried out to obtain results with improved quality. Wang et al. [12] reviewed current data fusion methods in surface metrology, and summarize the data fusion method into four categories which include repeated measurements, stitching, range image fusion, and 3D data fusion. Among these categories, the 3D data fusion is the most difficult task which involves complicated registration and fusion process, and may tackle datasets on different scales.

Ramasamy et al. [10] presented several scale decomposition based data fusion strategies and weighting methods in fusion of multi-scaled range images. Although the validity of the method has been proven on the measurement of micro-structured surfaces, the uncertainty propagation in fusion process is not known. Gaussian process was applied in data fusion of coordinate datasets [13, 14]. The method makes use of Gaussian process to model the geometry of the datasets, and the fusion is performed in a hierarchical approach by fusing the residuals of the datasets via repeated Gaussian processes. The application of the method is still limited to relatively simple surfaces and little research has been conducted on multi-scaled complex surfaces, and the time for the computation becomes infeasible when a large amount of data is involved [15]. Forbes et al [16] presented a weighted least square based multi-sensor data fusion method which uses a general Bayesian approach to balance the noise parameters by introducing weights to each datasets. The method relies on linear approximation of the geometry of the datasets, which may be problematic when the datasets have sharp geometrical changes. For instance, a smooth surface embedded with micro structures.

It is indicated from the literature that the surface modelling is one of the core techniques in data fusion process due to the different resolutions and distributions of the datasets. However, the geometric complexity of the multi-scale surfaces imposes a lot challenges in modelling and fusing the measured datasets [12]. This paper presents a reconstruction-registration integrated data fusion method to address this problem. The method divides the measured datasets into sub-datasets with different scales by fitting a common surface into the datasets via reconstruction and registration process so that the modelling and the fusion process are also decomposed. Data fusion is carried out among fitting and matching residuals of each datasets based on weighted mean with the aid of Gaussian process model. Comparison tests has been conducted with existing methods by both computer simulation and experimental work to verify the validity of the proposed method.

II. RECONSTRUCTION-REGISTRATION INTEGRATED DATA FUSION METHOD

As shown in Fig. 1, the proposed reconstruction-registration integrated data fusion (RRIDF) method performs the multi-scaled data fusion via reconstruction, registration, fusion, and merging process. It starts from reconstructing a continuous surface from one of the datasets. Appropriate error threshold should be enforced to balance the fitting accuracy and the surface smoothness. Based on surface reconstruction, the dataset, denoted as $\boldsymbol{D1}$, is divided into two sub-datasets, i.e. the reconstructed surface and its residuals, as given by

$$\boldsymbol{D1} = \boldsymbol{RS} + \boldsymbol{Res}_1 \tag{1}$$

where $\boldsymbol{RS}$ is the reconstructed surface; $\boldsymbol{Res}_1$ is the reconstruction residuals.

In the second step, another dataset, denoted as ***D2***, is transformed to the embedded coordinate frame of the ***D1*** based on surface registration. Hence, the ***D2*** can also be divided into two sub-datasets as given by

$$\boldsymbol{D2} = \boldsymbol{T}^{-1}\left(\boldsymbol{RS} + \boldsymbol{Res}_2\right) \tag{2}$$

where $\boldsymbol{T}$ is the coordinate transformation matrix evaluated in registration process; $\boldsymbol{Res}_2$ is the deviation of the transformed ***D2*** from ***RS*** and denoted as registration residuals. In the third step, the $\boldsymbol{Res}_1$ and the $\boldsymbol{Res}_2$ are fused via weighted mean process with the aid of Gaussian process modelling. In the forth step, the fused residuals are merged with the reconstructed surface ***RS*** to produce the final fusion result.

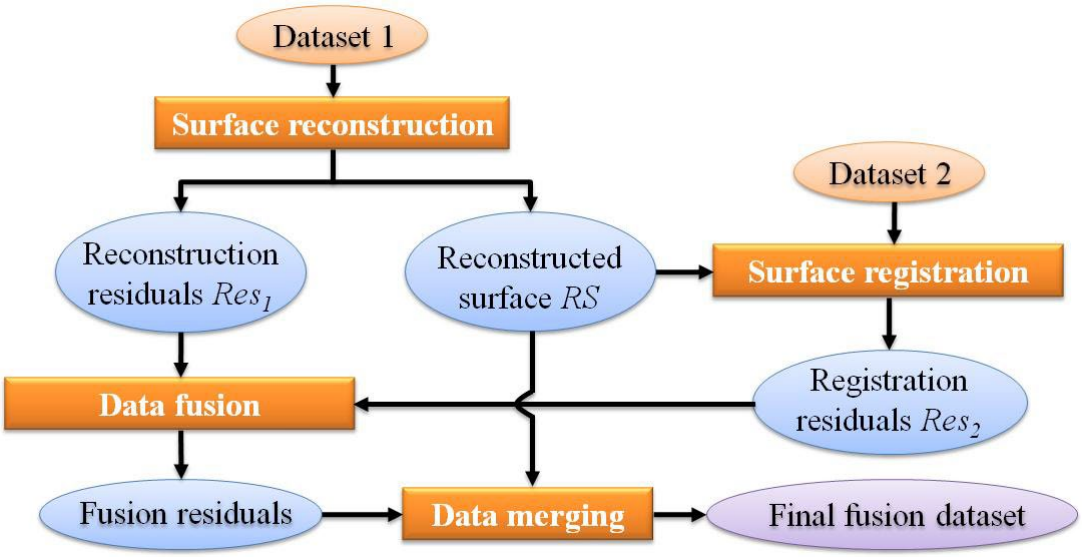

Fig. 1: Architecture of the multi-scale datasets fusion strategy

By fitting a common surface, the RRIDF method integrates the reconstruction and the registration process so that the multi-scaled features are decomposed into different scales in a common coordinate frame. This would benefit the consequent data fusion process since only the residuals regenerated in the reconstruction and the registration process are fused. Hence, the multi-scale modelling of complex features is avoided. In practice, the surface reconstruction should be carried out at the dataset which possesses lower resolution. This would further improve the registration accuracy since more correspondence pairs can be established during registration. The core algorithms of the data fusion process are given in details in following sections.

A. Surface Reconstruction

Due to the practically unlimited degree of geometric freedom and simple mathematics, B-spline surface is used to reconstruct a common surface from the dataset. A B-spline surface $\boldsymbol{S}$ is defined as [17]:

$$\boldsymbol{S}(u,v) = \sum_{i=0}^{i=n_u-1}\sum_{j=0}^{j=n_v-1} N_{i,p}(u)N_{j,q}(v)\boldsymbol{P}_{ij} \tag{3}$$

where $\boldsymbol{P}_{ij}$ is the control point controlling the shape of the surface; n_u and n_v are the numbers of control points in u and v direction respectively; u and v are surface parameters identifying the location of point $\boldsymbol{S}(u,v)$ within the length of the two directions of the surface; $N_{i,p}(u)$ and $N_{j,q}(v)$ are the normalized B-spline functions uniquely defined by the degree p and knot vector U, degree q and knot vector V, respectively. Eq. (3) can further be simplified to Eq. (4) as follows:

$$\boldsymbol{S}(u,v) = \sum_{s=0}^{n_c-1} N_s(u,v)\boldsymbol{P}_s = \boldsymbol{NP} \tag{4}$$

where

$$n_c = n_u n_v, \quad \boldsymbol{P}_s = \boldsymbol{P}_{i(s),j(s)},$$

$$N_s(u,v) = N_{i(s),p}(u)N_{j(s),q}(v), \quad i(s) = \left\lfloor \frac{s}{n_v} \right\rfloor, \; j(s) = s \bmod n_v$$

$\boldsymbol{N} = \left(N_{s-1}(u_k, v_k)\right)_{k,s} \in \mathbb{R}^{m \times n_c}$ is the matrix of base function, $\boldsymbol{P} = \left(\boldsymbol{P}_1, ..., \boldsymbol{P}_{n_c}\right)^T \in \mathbb{R}^{n_c \times 3}$ is the matrix of control point. Substituting Eq. (4) to Eq. (1), a B-spline surface model can be obtained:

$$\boldsymbol{D1} = \boldsymbol{NP} + \boldsymbol{Res_1} \tag{5}$$

Control points $\boldsymbol{P}$ is determined such that the objective function

$$F = \left\| \boldsymbol{NP} - \boldsymbol{D1} \right\|^2 \tag{6}$$

is minimized by vanishing the partial derivative of F to it, as shown in Eq. (7).

$$\boldsymbol{P} = \left(\boldsymbol{N}^T \boldsymbol{N}\right)^{-1} \boldsymbol{N}^T \boldsymbol{D1} \tag{7}$$

$\boldsymbol{Res}_1$ is then determined by projecting the $\boldsymbol{D1}$ to the reconstructed surface along Z axis. In practice, the unknown parameters and the knot vectors are determined by constructing a simple initial surface [18], and the number of the control points is determined iteratively for given error threshold. The error threshold is determined in such a way that the reconstructed surface well represents the geometry of the surface for accurate surface registration in following process, while overfitting should be also avoid as well to limit the number of the parameters involved in the surface model and maintain computational efficiency. More details can be referred to the work presented by M.J. Ren et al [18]. It is worthy to note that the reconstruction accuracy has limited influence to the fusion since the residuals will be fused into the final result.

B. Surface Registration

In the multi-sensor system, the measured datasets may be embedded in their own sensor coordinate systems, and the elimination of the misalignment of the coordinate frame must be carried out before data fusion. Registration of two datasets can be formulated as an optimization problem as given in Eq. (8) which

searches for an optimal Euclidean motion that the two datasets are aligned as closely as possible at the overlapping area, and the error metric of the alignment is described by the sum of the square distance of the two datasets at each point as given by Eq. (8) [19].

$$F = \min\left(\sum_{i=1}^{N} \left| \boldsymbol{RS}_i - T\left(\boldsymbol{m}\right) \boldsymbol{D2}_i \right|^2 \right) \tag{8}$$

where $\boldsymbol{D2}_i$ is a point of $\boldsymbol{D2}$; $\boldsymbol{RS}_i$ is the corresponding point of $\boldsymbol{D2}_i$ on $\boldsymbol{RS}$; $\boldsymbol{T}(m)$ is the function of the coordinate transformation matrix by taking the spatial parameters $\boldsymbol{m}$ as variable. $\boldsymbol{m}$ contains three translational offsets and three rotational angles. The corresponding point $\boldsymbol{RS}_i$ can be determined by projecting the $\boldsymbol{D2}_i$ on $\boldsymbol{RS}$ since a continuous surface is reconstructed on $\boldsymbol{D1}$. Hence, the registration is conducted in a nested approach. It starts from establishing the corresponding pairs ($\boldsymbol{D2}_i$, $\boldsymbol{RS}_i$) in inner iteration, and the coordinate transformation matrix is determined in the outer iteration based on Eq. (8).

The coordinate transformation matrix $\boldsymbol{T}(m)$ is determined by the local minima of Eq. (8) as follows:

$$\frac{\partial F}{\partial \boldsymbol{m}} = 2\left(\boldsymbol{RS} - \boldsymbol{TD2}\right)' \frac{\partial\left(\boldsymbol{RS} - \boldsymbol{TD2}\right)}{\partial \boldsymbol{m}} = 0 \tag{9}$$

where $\boldsymbol{RS} = \left[RS_1, \ldots, RS_N\right]$ and $\boldsymbol{D2} = \left[D2_1, \ldots, D2_N\right]$ are 4N×1 matrix, $\boldsymbol{T}$ is $4N\times4N$ identity matrix. Eq. (9) can be solved by using Levenberg-Marquardt algorithm [20]. It starts from a given parameters and the increment in each iteration is determined as follows:

$$\delta \boldsymbol{m} = -\left[\boldsymbol{J}^T \boldsymbol{J} + \lambda \boldsymbol{D}\right]^{-1} \boldsymbol{J}^T \boldsymbol{m} \tag{10}$$

where $\boldsymbol{D}$ is the 6×6 identity matrix; $\partial\left(\overline{\boldsymbol{P}} - \overline{\boldsymbol{TQ}}\right)/\partial \boldsymbol{m}$ is 4N×6 Jacobi matrix; λ is a damping factor.

C. Weighted mean fusion based on Gaussian process model

In the present study, a weighted mean is taken on the fused datasets so that fusion results with reduced uncertainty can be obtained. Suppose $z_{1,i}$ and $z_{2,i}$ are values of $\boldsymbol{Res_1}$ and $\boldsymbol{Res_2}$ at (x_i, y_i) with associated uncertainties σ_1 and σ_2 respectively. Hence, the weighted mean fusion of the two values is given by Eq. (11),

$$z_{f,i} = w_1 z_{1,i} + w_2 z_{2,i} \qquad s.t. \quad w_1 + w_2 = 1 \tag{11}$$

where w_1 and w_2 are the weight of each dataset. The uncertainty of the fusion result z_f, denoted by σ_f, can be determined as follows:

$$\sigma_f^2 = w_1^2 \sigma_1^2 + w_2^2 \sigma_2^2 \tag{12}$$

Hence, the w_1 and w_2 can be determined by minimizing the uncertainty of the fusion result σ_f^2, and can be calculated as

$$w_1 = \frac{\sigma_2^2}{\sigma_1^2 + \sigma_2^2} \quad , \qquad w_2 = \frac{\sigma_1^2}{\sigma_1^2 + \sigma_2^2} \tag{13}$$

Due to different resolutions and distributions, one of the residuals should be modelled so that point-wise manner can be performed via a re-sampling process. To maintain higher resolution and efficiency, the dataset possessing lower resolution is modeled based on Gaussian process (GP) model [21]. GP is a Bayesian regression model which can be completely specified by a mean function $\mu(\boldsymbol{X})$ and covariance function $K(\boldsymbol{X}, \boldsymbol{X})$ as given by Eq. (14).

$$f(\boldsymbol{X}) \sim N\left(\mu(\boldsymbol{X}), K(\boldsymbol{X}, \boldsymbol{X})\right) \tag{14}$$

In actual measurement, zero-offset mean function is used since no prior knowledge on the surface geometry is available. A prediction m and its uncertainty cov at an arbitrary location $\boldsymbol{x}$ on the model can then be obtained from the marginal distribution of $f(\boldsymbol{x})$ as follows [21]:

$$m = K\left(\boldsymbol{x}, \boldsymbol{X}\right)\left(K\left(\boldsymbol{X}, \boldsymbol{X}\right) + \sigma_\varepsilon^2 I\right)^{-1} \boldsymbol{Z} \tag{15}$$

$$cov = K\left(\boldsymbol{x}, \boldsymbol{x}\right) - K\left(\boldsymbol{x}, \boldsymbol{X}\right)\left(K\left(\boldsymbol{X}, \boldsymbol{X}\right) + \sigma_\varepsilon^2 I\right)^{-1} K\left(\boldsymbol{X}, \boldsymbol{x}\right) \tag{16}$$

It can be inferred from the definition of the GP that the covariance function provides the correlation among any set of outputs and forms the beating heart of GP model. In the present study, squared exponential function and Martern class functions are alternatively used to deal with different kinds of surface topographies [8]. Hence, Eq. (15) and Eq. (16) can be incorporated into Eq. (11) to perform the weighted mean fusion of the residuals. For more details regarding to the GP modelling can be referred to the work presented by C.E. Rasmussen et al [21].

III. EXPERIMENTAL STUDY

The proposed RRIDF method has been implemented and tested for variety of surfaces with various complexities. Case studies on three typical multi-scaled surfaces in advanced optics are presented by computer simulation and actual measurement to examine the validity of the proposed method.

A. Computer simulation

Three multi-scaled complex surfaces are generated by superimposing micro lens arrays, micro pyramid arrays, and sinusoidal waves on different substrate surfaces. The micro lens arrays and its substrate surface is defined by Eq. (17).

$$z = \sin\left(0.5x\right) + \cos\left(0.5y\right) - \sqrt{R^2 - \left(x - x_i\right)^2 + \left(y - y_i\right)^2} - h \tag{17}$$

where $x, y \in [-2\pi, 2\pi]$; (x_i, y_i), $R = 2.5mm$, and $h = 2.45mm$ are the location, radius, and offset of each lens. The pyramid arrays share the same substrate surface with lens arrays. They are four sided, and the height and width of each pyramid are 0.05 mm and 1 mm, respectively. The sinusoidal waves and its substrate surface is defined by Eq. (18).

$$z = -0.01x^2 - 0.01y^2 + 0.15\cos(2x) + 0.15\cos(2y) \tag{18}$$

where $x, y \in [-10, 10]$ mm. Fig. 2 shows the three generated multi-scaled surfaces.

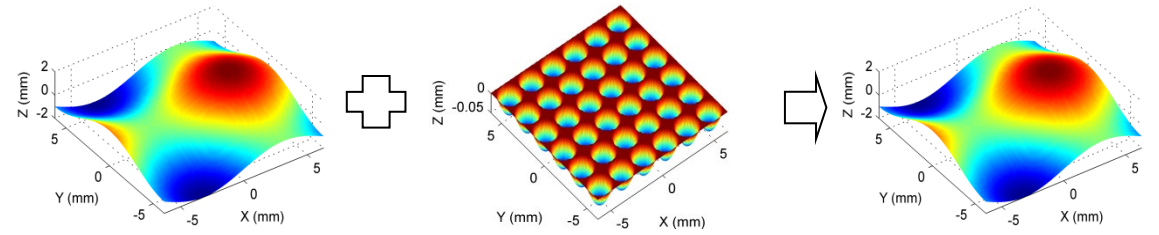

(a) micro lens arrays superimposed on a sinusoidal freeform surface

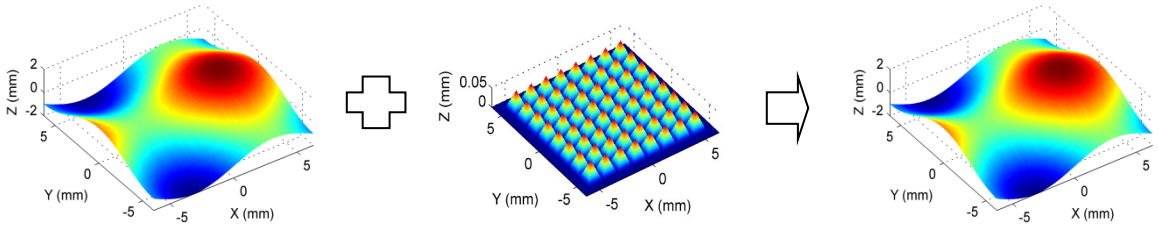

(b) micro pyramid arrays superimposed on a sinusoidal freeform surface

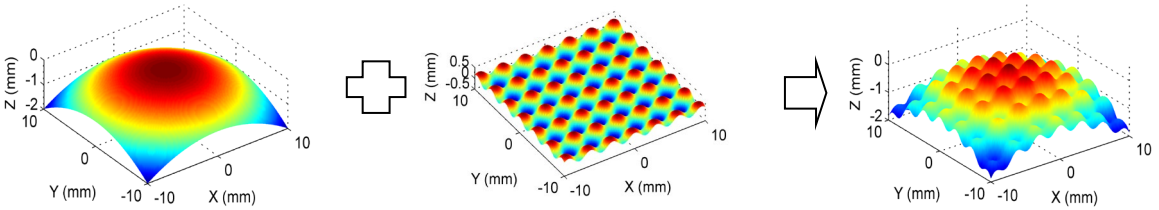

(c) Sinusoidal waves superimposed on a parabola

Fig. 2: Designed three different multi-scaled complex surfaces

In each case study, multi-sensor datasets are simulated by uniformly sampling two sets of data from corresponding designed surfaces, and denoted as ***D1*** and ***D2***. For micro lens arrays and pyramid arrays, ***D1*** and ***D2*** are sampled with spacing 0.4mm and 0.1mm, respectively. For sinusoidal waves, ***D1*** and ***D2*** are with spacing 1 mm and 0.2 mm, respectively. ***D1*** and ***D2*** are added Gaussian noise with standard deviation 1μm and 5μm respectively to represent the measurement errors. The dataset ***D2*** is moved to an arbitrary position to produce the misalignment of the coordinate frames of the two datasets. Hence, two datasets are a combination of low resolution with high accurate dataset and high resolution with low accurate dataset, which is very common in multi-sensor surface metrology to balance the measurement efficiency and accuracy. It is noted that ***D1*** and ***D2*** have different resolutions with different associated uncertainties and are

embedded in different coordinate frames. The proposed RRIDF method is then used to fuse the ***D1*** and ***D2*** to obtain a unique representation of the surfaces.

Fig. 3 shows the process of the RRIDF method in fusing the datasets of micro lens arrays as an example. It starts from reconstructing a smooth surface from the dataset ***D1*** to decompose the dataset into two different scales of sub-datasets. Secondly, dataset ***D2*** is transformed to the coordinate frame of ***D1*** via surface registration. Hence, ***D2*** is also decomposed into two different scales, while share the same common surface. Thirdly, Gaussian process (GP) model is used to fit the residuals of ***D1***. A set of points are re-sampled on the established GP model in according to the resolution of the ***D2***.

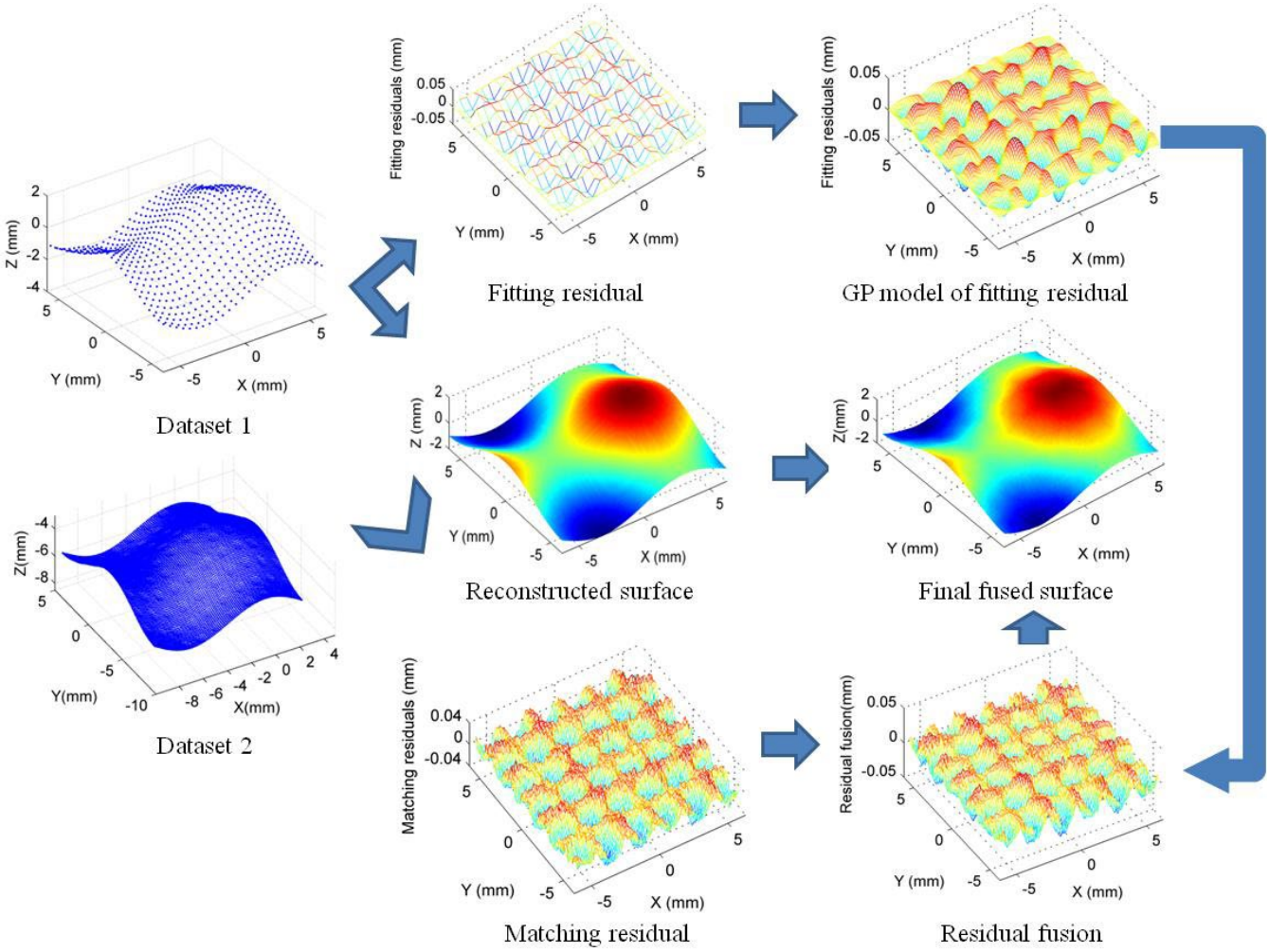

Fig. 3: Multi-scale datasets fusion process

Fig. 4 shows the estimated uncertainty of the established GP model. It is clearly shown in Fig. 4 that the regions near by the fitted data points possess higher uncertainty than the regions far away from the fitted data. The characteristics of the uncertainty distribution are used in data fusion via weighted mean process so that the effect of the fitting error generated in re-sampling process can be restricted, and a fusion result with

improved quality can be expected. Finally, the fusion result of the two residual terms is merged on the reconstructed surface to generate the final fusion dataset.

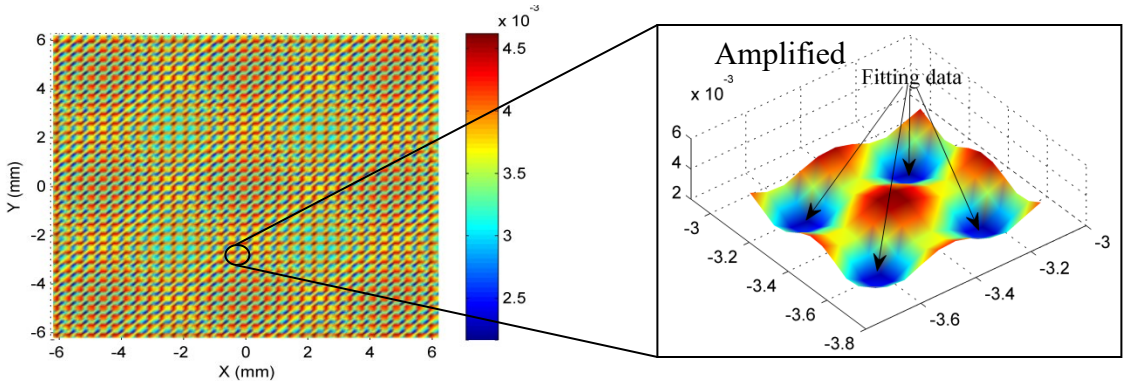

Fig. 4: Estimated uncertainty of the established GP model (unit in *mm*)

Registration process is repeated 100 times to evaluate the accuracy of the RRIDF method. Fig. 5 shows the uncertainty of the evaluated 6 spatial parameters, including three rotational angles rx, ry, rz, and three translation offsets tx, ty, tz, respectively. The results are compared with that are obtained by classical Iterative Closest Point method [11]. The results indicate that the performance of the proposed method well matches with that of the ICP method and possesses slightly lower uncertainty. This is due to the fact that the surface reconstruction process not only rejects the noise of the one of the registered datasets but also creates larger number of correspondences in registration process.

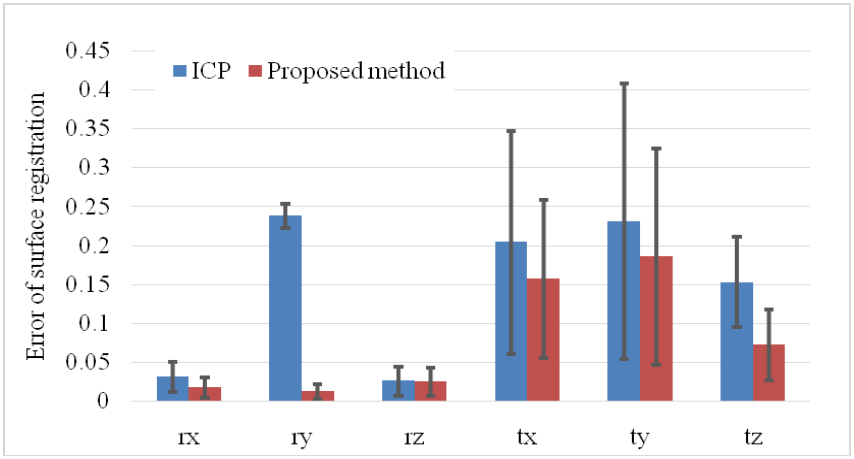

Fig. 5: Error of evaluated spatial parameters (rx, ry, rz are in µrad, tx, ty, tz are in µm)

To evaluate the performance of the RRIDF method in fusing 3D datasets, comparison tests have been conducted with two existing methods, namely Gaussian process based data fusion method (GPDF) [14] and weighted least square based data fusion method (WLSDF) [16]. Both of two methods are reported having capability in fusing 3D datasets with improved quality, which has also been reviewed in Section I. All the three methods are implemented on MATLAB and run on an Intel Core i5-3470 CPU with 4.0 GB of RAM.

Table 1 summarizes the fusion results of the three methods on three designed surfaces, respectively. Three parameters are used to characterize the performance of the fusion methods, including running time, peak-to-valley (PV) error, and root-mean-square (RMS) error of the fused datasets. The PV and RMS of the original datasets are around 37μm and 5μm respectively, and are used as benchmark in all case studies.

Table 1: A summary of comparison test of three fusion methods on three designed surfaces

	Micro lens arrays			**Micro pyramid arrays**			**Sinusoidal waves**		
	RRIDF	**GPDF**	**WLSDF**	**RRIDF**	**GPDF**	**WLSDF**	**RRIDF**	**GPDF**	**WLSDF**
PV (μm)	16.9	16.7	23.8	19.6	19.3	25.7	7.6	7.1	10.4
RMS (μm)	2.1	2.1	3.4	2.3	2.2	3.9	0.9	0.8	1.2
Time (s)	17.2	>3600	16.3	17.3	>3600	16.6	15.6	>3600	14.5

It is shown in the results that all the methods are capable of fusing datasets with improved quality, while the proposed RRIDF method and the GPDF method possess better accuracy than the WLSDF method, especially when the fused datasets contains sharp features. As pointed out in Section I, WLS method relies on linear approximation of the geometry of the datasets, which may be problematic when the datasets have sharp geometrical changes. Fig. 6 and Fig. 7 show examples of the error maps of the fused datasets obtained by the RRIDF method and WLSDF method. It is observed that the error maps of the fused datasets obtained by the RRIDF method shows strong random behavior which clearly results from the added noise, and no specific systematic pattern has been observed even at the edges of the micro elements. On the other hands, the fused datasets obtained by the WLSDF method has large errors at the edges of the micro elements, which inevitably results in systematic errors to the results. It is also observed that the WLSDF method has much better performance in fusing smooth datasets. However, the proposed RRIDF still has better accuracy than WLSDF. The statistic nature of the GP leads superior performance than WLSDF in learning and rejecting the random error associated in the datasets in the modelling process, as shown in Fig. 8. This demonstrates the capability of the proposed method in modelling and fusing multi-scaled complex datasets.

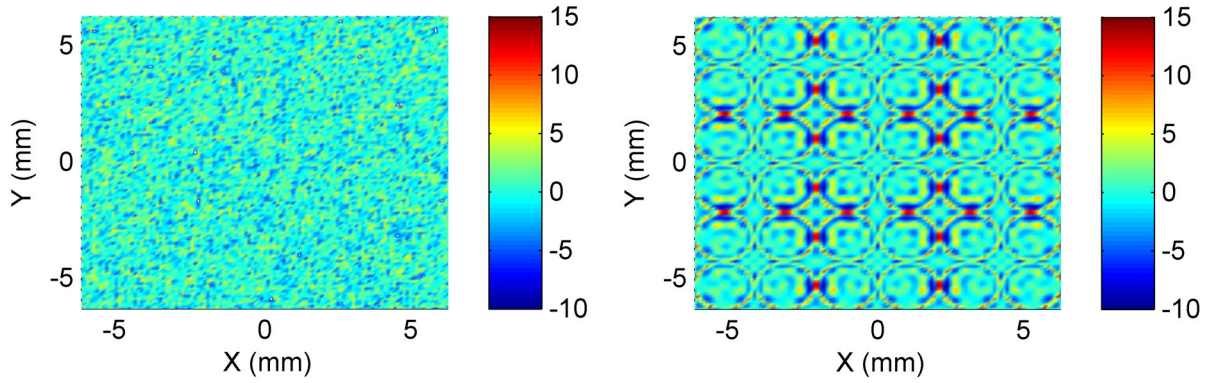

(a) Error fusion dataset by RRIDF method (b) Error fusion dataset by WLSDF method

Fig. 6: Error map comparison of fusion datasets of micro lens arrays (unit in μm)

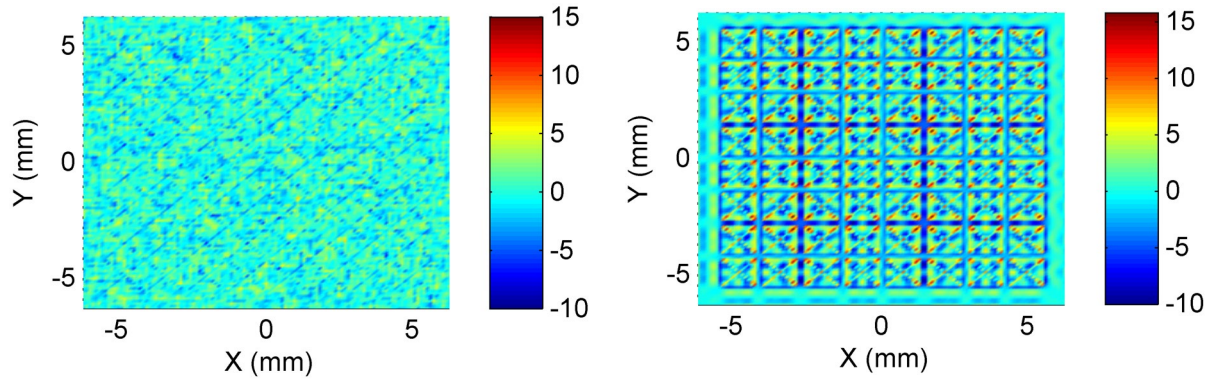

(a) Error fusion dataset by RRIDF method (b) Error fusion dataset by WLSDF method

Fig. 7: Error map comparison of fusion datasets of micro pyramid arrays (unit in μm)

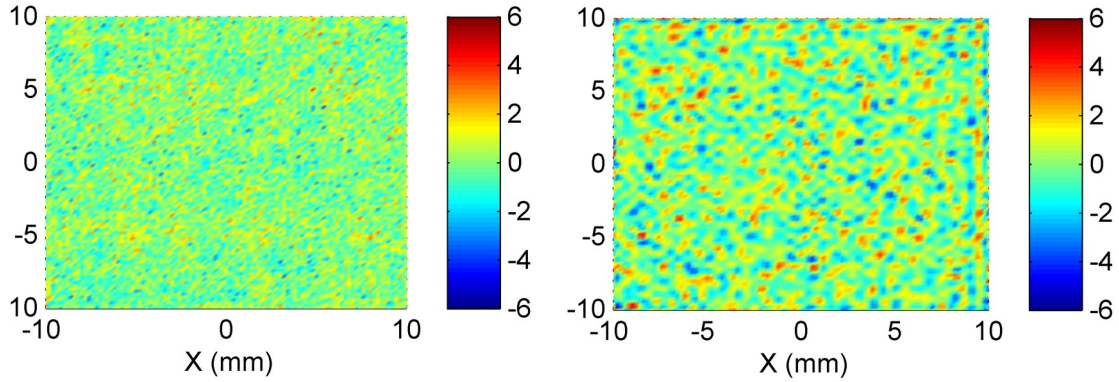

(a) Error fusion dataset by RRIDF method (b) Error fusion dataset by WLSDF method

Fig. 8: Error map comparison of fusion datasets of sinusoidal waves (unit in μm)

Both of the proposed RRIDF method and the GPDF method use the GP as a mathematical foundation to model the surface geometry. It is noted that GP modelling of multi-scaled surfaces requires adequate number of points to establish an accurate model. For the GPDF method, owing to the complexity of the surfaces, it requires modelling both the two datasets ***D1*** and ***D2*** in the fusion process [14] so that an accurate GP model can be established. Although slightly better fusion quality has been obtained, the fusion process costs several hours for the computation. This is due to the reason that the computation complexity of the GP modelling is $O(N^3)$ and it normally requires hundreds of iterations in refining the established model. Since the dataset ***D2*** has a large number of points, the time for the computation becomes infeasible. For the proposed method, by decomposing the datasets into different scales, only the residuals of the dataset ***D1*** which possesses relatively little data has been modelled by the GP and the fusion is performed based on weighted mean process so that same level of accuracy has been obtained with much lower computation cost. It is interesting to note from the

comparison tests that both the enhanced registration accuracy and fusion quality are achieved by the proposed method with acceptable computation cost.

It is also worthy to note that the RRIDF method still relies on adequate number of sampling points. Inadequate number of sampling points would make the RRIDF method generate errors in surface reconstruction and GP modelling. The errors should be considered as insufficient sampling errors. Regardless of the data fusion methods being used, including the RRIDF, GPDF, and WLSDF, the error caused by the insufficient sampling would inevitably propagate to the final fusion dataset. Hence, it is important to design appropriate sampling strategy to limit the sampling errors to an acceptable level based on required measurement accuracy. Optimal design of the sampling strategy for complex surfaces is however difficult and is normally performed adaptively in the measurement process based on some surface modelling methods [22]. From this point of view, the proposed RRIDF method can be served as a surface modelling method to perform adaptive sampling of the complex surfaces on multi-sensor systems. For more details regarding the sampling issues can be found elsewhere [22].

B. Actual Measurement

The designed sinusoidal waves are machined to further evaluate the performance of the proposed RRIDF method in actual measurement. Two different sensors including a high precision CMM Hexagon Leitz PMM-Xi and a Keyence LK-laser scanner are used in the experiments. The CMM possesses length measurement uncertainty with U=(0.6+L/500, L in mm) μm, and the probing error with u=0.9μm (1σ, normal). The uncertainty of the laser scanner is identified to be u=3.4μm (1σ, normal) by a reference ball. Before the multi-sensor experiment, CMM is used to measure the surface with 0.5 mm spacing over the entire surface. A total of 1600 points were measured and were used to evaluate the form error of the measure surface [19]. Fig. 9 shows the measurement process and the measured surface. The PV and RMS of the measured surface are identified to be 9.9μm and 1.9μm respectively. The whole process takes several hours, and hence the time for the measurement is expensive.

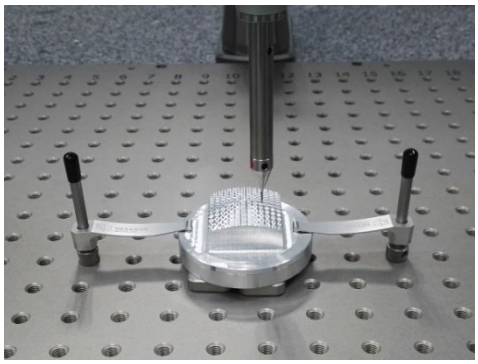

(a) Measurement process

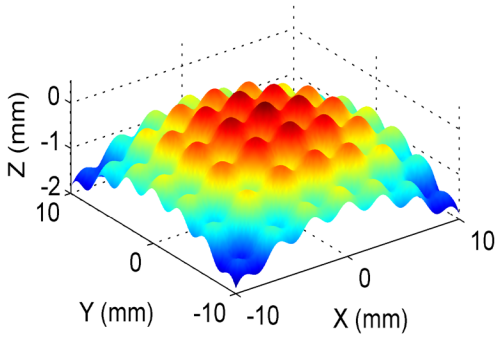

(b) Measured surface

Fig. 9: Measurement of a machined sinusoidal waved multi-scale surface

To realize both high efficient and high accurate performance, Keyence LK-laser scanner is incorporated into the process to perform corporative measurement of the mould insert. The measurement has been carried out in two steps. In the first step, the laser scanner was used to measure the workpiece. Approximately 10000 points were uniformly sampled with a spacing 0.2mm in both X direction and Y direction in several minutes. The measured result is considered to be a high resolution and low accurate dataset, and denoted as ***ED2***. Secondly, CMM is used to measure the workpiece with a spacing of 1 mm. A total of 400 points were measured with uniform sampling over the entire surface, which is considered to be low resolution and high accurate dataset as denoted by ***ED1***. The whole measurement process takes approximately half an hour. The proposed RRIDF method is then used to fuse the datasets, and the results are also compared with that are obtained by the GPDF method and the WLSDF method.

It starts from the reconstruction of a smooth surface from ***ED1***, and the residuals are modelled by GP. The reconstructed surface is matched with the ***ED2***, and the resulting residuals are then fused with the GP model of the fitting residual for ***ED1***. The fusion residual is then merged with the reconstructed surface to form the final fusion dataset, and denoted to be ***EDf***. Fig. 10 shows the evaluated form error of the ***EDf*** obtained by the RRIDF method, the GPDF method, and the WLSDF method, respectively, and a summary of the evaluated parameters are given in Table 2. They are also compared with the benchmarking obtained in earlier step. The results show that the RRIDF method and the GPDF method achieved very similar form errors and they all have superior performance than WLSDF method in terms of fusion accuracy, which is in accordance with the simulation results. However, the GPDF method takes more than 1 hour in fusing the two datasets, which makes it less practical in actual application. It is interesting to note that, based on the RRIDF method, the multi-sensor measurement strategy obtained the similar level of accuracy in much short measurement duration as comparing with that are obtained by the CMM dense measurement. This further demonstrates the capability of the proposed method in fusing multi-sensor datasets.

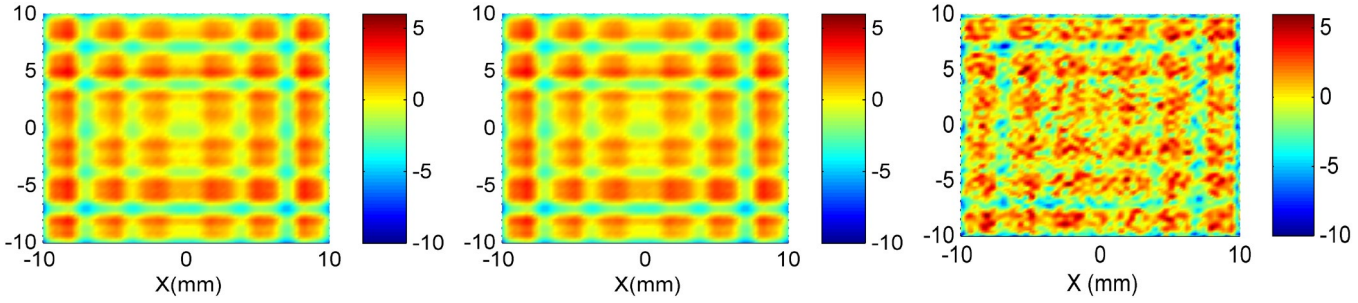

(a) results of RRIDF method (b) results of RRIDF method (c) results of WLSDF method

Fig. 10: Comparison of uncertainty in GP fusion (unit in μm)

Table 2: A summary of form error evaluation results

	Benchmarking	RRIDF method	GPDF	WLSDF method
PV (μm)	9.9	10.5	10.3	13.1
RMS (μm)	1.9	2.0	2.0	2.2

IV. CONCLUSION

This paper presents a reconstruction-registration integrated data fusion method for the measurement of multi-scaled complex surfaces. To overcome the difficulty in modelling and fusing of multi-scaled complex datasets, the method integrates the reconstruction and registration process to decompose the datasets into different scales of sub-datasets so that the multi-scale modelling and fusion process are also decomposed and are carried out based on weighted mean method with the aid of Gaussian process model. Experimental study demonstrates that the superior performance of the proposed method in terms of both high efficiency and accuracy. In future work, the method will be incorporated into multi-sensor systems and used as mathematical foundation for the design of optimal multi-sensor measurement strategy so as to improve the metrological performance in measuring complex surfaces.

ACKNOWLEDGMENT

The work was supported by the National Natural Science Foundation of China (No. 51505404), China National Program on Key Basic Research Project (No. 2011CB013203) and the Research Grants Council of the Government of the Hong Kong Special Administrative Region, China under the project No.15202814. The work was also supported by a PhD studentship (project account code: RTHC) from The Hong Kong Polytechnic University.

REFERENCES

[1] E. Brinksmeier, L. Schonemann, “Generation of discontinuous microstructures by diamond micro chiseling”, *CIRP Ann-Manuf. Tech.*, vol. 63, pp.49-52, 2014.

[2] X. Jiang, D.J. Whitehouse, “Technological shifts in surface metrology”, *CIRP Ann-Manuf. Tech.*, vol. 61, pp.815-836, 2012.

[3] D.J. Whitehouse, “Surface geometry, miniaturization and metrology”, *Phil. Trans. R. Soc. A*, vol. 370, pp.4042-4065, 2012.

[4] R. Leach, R. Boyd, T. Burke, H.U. Danzebrink, K. Dirscherl, T. Dziomba, M. Gee, L. Koenders, V. Morazzani, A. Pidduck, D. Roy, W.E. Unger, A. Yacoot, “The European nanometrology landscape”, *Nanotechnology*, vol. 22, pp. 062001, 2011.

[5] A. Weckenmann, G. Peggs, J. Hoffmann, "Probing systems for dimensional micro- and nano-metrology", *Meas. Sci Technol.*, vol. 17, pp. 504-509, 2006.

[6] A. Weckenmann, A. Schuler, "Application of modern high resolution tactile sensors for micro-objects", International Journal of Precision Technology 2, 266-288 (2011).

[7] Werth Messtechnik GmbH, http://www.werthmesstechnik.de, accessed in Mar. 31th 2016.

[8] Witec GmbH, http://www.witec.de/products/, accessed in Mar. 31th 2016.

[9] A. Weckenmann, X. Jiang, K. Sommer, U. Newschaefer-Rube, J. Seewig, L. Shaw, T. Estler, "Multisensor data fusion in dimensional metrology", *CIRP Ann-Manuf. Tech.*, vol. 58, pp. 701-721, 2009.

[10] S.K. Ramasamy, "Multi-scale data fusion for surface metrology", *PhD thesis*, the University of North Carolina at Charlotte, USA, 2011.

[11] P.J. Besl, N.D. McKay, "A method for registration of 3D shapes", *IEEE T. Pattern Anal.*, vol. 14, pp. 239-256, 1992.

[12] J. Wang, R. Leach, X. Jiang, "Review of the mathematical foundations of data fusion techniques in surface metrology", *Surf. Topogr.: Metrol. Prop.*, vol. 3, pp. 023001, 2015.

[13] Z.G. Qian and C.F. Wu, "Bayesian hierarchical modeling for integrating low-accuracy and high-accuracy experiments", *Technometrics*, Vol. 50, pp. 192-204, 2008.

[14] B.M. Colosimo, M. Pacella, N. Senin, "Multi-sensor data fusion via Gaussian process models for dimensional and geometric verification", *Precision Engineering*, vol. 40, pp. 199-213, 2015.

[15] C.E. Rasmussen, C.K.I. Williams, "Gaussian processes for machining learning", Cambridge, Mass.: MIT Press, 2006.

[16] A.B. Forbes, "Weighting observations from multi-sensor coordinate measuring systems", *Meas. Sci. Technol.*, vol. 23, pp. 025004, 2012.

[17] L. Piegl, W. Tiller, "The NURBS book", Springer-Verlag, Berlin, 1997.

[18] M.J. Ren, C.F. Cheung, L.B. Kong, "A robust surface fitting and reconstruction algorithm for form characterization of ultra-precision freeform surfaces," *Measurement*, vol. 44, pp.2068-2077, 2011.

[19] M.J. Ren, C.F. Cheung, L.B. Kong, J. Jiang, "Invariant feature pattern based form characterization for the measurement of ultra-precision freeform surfaces," *IEEE T Instrum. Meas.*, vol. 61, pp. 963-973, 2012.

[20] D.W. Marquardt, "An algorithm for least squares estimation of nonlinear parameters", *J. Soc. Ind. Appl. Match,* vol. 11, pp. 431-441, 1963.

[21] C.E. Rasmussen, C.K.I. Williams, "Gaussian processes for machining learning", Mass.: MIT Press, Cambridge, 2006

[22] J. Wang, R.K. Leach, X. Jiang, “Advances in sampling techniques for surface topography measurement – a review”, *NPL Report*, ENG 55, 2014.